Efficient Approach to Solving Transient Unsaturated Flow Problems. II: Numerical Solutions

André Luís Brasil Cavalcante, Ph.D.[1]; and Jorge Gabriel Zornberg, Ph.D.[2]

Abstract: Although the finite-difference method (FDM) has been commonly used to numerically solve Richard's equation, numerical difficulties are often encountered, even for comparatively simple problems. To minimize convergence problems, comparatively small discretization and time steps have often been adopted to solve this highly nonlinear equation, resulting in significant computational costs. To overcome these difficulties, this paper presents an efficient approach to solving Richard's equation that combines two numerical techniques: the FDM and the cubic interpolated pseudoparticle (CIP) method. The FDM is used to solving the diffusive flow component of Richard's equation, the convergence of which can be controlled by adopting time steps corresponding to Neumann's number under 0.5. In contrast, the CIP method is used to solve the advective flow component of the equation. The CIP method is found to be particularly suitable for facilitating convergence and eliminating the presence of spurious results when the Courant number is under 1.0. Analytical solutions for transient unsaturated flow problems, developed in a companion paper, allow comparison between the predictions obtained using the proposed numerical approach and the exact solutions. Use of the newly developed algorithm is found to be particularly accurate and stable for solving Richard's equation, being clearly superior to the use of the traditional FDM. After validating the new numerical approach using the boundary conditions and hydraulic functions for which analytical solutions have been developed, the new numerical scheme was subsequently implemented to address more general unsaturated flow problems. In particular, the new numerical approach was extended to solve unsaturated flow problems involving complex soil hydraulic functions as well as different boundary conditions. Comparisons are presented to illustrate the accuracy of the new numerical approach even when extended to incorporate the use of complex hydraulic functions for which there are no analytical solutions. The efficient, validated numerical schemes presented in this paper are found to be well suited for solving complex unsaturated flow problems. **DOI: 10.1061/(ASCE)GM.1943-5622.0000876.**

Author keywords: Unsaturated flow; Richard's equation; Numerical model; Cubic interpolated pseudoparticle (CIP); Advection; Diffusion.

Introduction

Transient unsaturated flow problems can be solved using Richard's equation (Richards 1931), which results from considering continuity and the validity of Darcy-Buckingham's law. This is a transient, nonlinear partial differential equation that contains a hyperbolic (gravitational) term and involves highly nonlinear hydraulic functions that may be spatially variable. Numerical solutions of Richard's equation have been challenging to implement because of the highly nonlinear nature of the soil hydraulic functions, including the soil water retention curve (SWRC) and the hydraulic conductivity function (k-function). Also because of these difficulties, analytical solutions to transient unsaturated flow problems have not been readily available, which has prevented a thorough comparison between analytical results and numerical predictions.

The most common representation of Richard's equation, for the case of one-dimensional unsaturated transient flow under a natural gravitational field in the z-direction, is

$$\frac{\partial \theta}{\partial t} = \frac{\partial}{\partial z}\left[k_z(\psi)\left(\frac{1}{\rho_w g}\frac{\partial \psi}{\partial z} - 1\right)\right] \tag{1}$$

where θ = volumetric water content (L^3/L^3); ψ = suction (using atmospheric pressure as reference) ($ML^{-1}T^{-2}$); ρ_w = fluid density (ML^{-3}); $k_z(\psi)$ = unsaturated hydraulic conductivity in the z-direction (k-function) expressed in terms of ψ (L/T); g = acceleration of gravity (L/T^2); and t = time (T).

An additional representation of Richard's equation is its θ-based version, also known as the Fokker-Planck equation (Philip 1969; Bear 1979), as follows:

$$\frac{\partial \theta}{\partial t} = \frac{\partial}{\partial z}\left[D_z(\theta)\frac{\partial \theta}{\partial z}\right] - \frac{\partial k_z(\theta)}{\partial z} \tag{2}$$

with

$$D_z(\theta) = \frac{k_z(\theta)}{\rho_w g}\frac{\partial \psi}{\partial \theta} \tag{3}$$

where D_z = unsaturated water diffusivity in the z-direction (L^2/T).

Cavalcante and Zornberg (2017) used a different form of the θ-based version of Richard's equation, which was particularly suitable to obtain analytical solutions to transient unsaturated flow problems. The revised form of the θ-based Richard's equation is

[1]Associate Professor, Dept. of Civil and Environmental Engineering, Univ. of Brasília, Brasília-DF 70910-900, Brazil (corresponding author). ORCID: http://orcid.org/0000-0002-7104-0371. E-mail: abrasil@unb.br

[2]Professor, Dept. of Civil Architectural and Environmental Engineering, Univ. of Texas, Austin, TX 78712-0280. E-mail: zornberg@mail.utexas.edu

Note. This manuscript was submitted on April 18, 2016; approved on November 4, 2016; published online on February 6, 2017. Discussion period open until July 6, 2017; separate discussions must be submitted for individual papers. This paper is part of the ***International Journal of Geomechanics***, © ASCE, ISSN 1532-3641.

$$\frac{\partial \theta}{\partial t} = \frac{\partial}{\partial z}\left[D_z(\theta)\frac{\partial \theta}{\partial z}\right] - a_s(\theta)\frac{\partial \theta}{\partial z} \tag{4}$$

with

$$a_s(\theta) = \frac{\partial k_z(\theta)}{\partial \theta} \tag{5}$$

where $a_s(\theta)$ = unsaturated advective seepage (L/T). A relevant aspect of the revised representation of Richard's equation is that it facilitates interpretation of unsaturated flow as a process that involves advective and diffusive flow components. Using this representation of Richard's equation and specific hydraulic functions, Cavalcante and Zornberg (2017) developed analytical solutions for transient unsaturated flow problems using a variety of boundary conditions.

This paper presents the development of new numerical schemes for solving Richard's equation for unsaturated flow problems under transient conditions. The new numerical scheme benefits from three important aspects: (1) the representation of Richard's equation in terms of advective and diffusive components [Eq. (4)], (2) the use of a particularly efficient numerical technique to solve the advective flow component, and (3) the availability of recently developed analytical solutions that allow comparison between numerical predictions and exact solutions. Comparisons between numerical and analytical results are conducted for a variety of boundary conditions, including a constant moisture imposed on the upper boundary of a soil column (semi-infinite and finite-length cases) as well as a constant discharge velocity imposed on the upper boundary of a soil column (semi-infinite and finite-length cases).

Efficient Numerical Scheme for Solving Transient Unsaturated Flow Problems

Although the finite-difference method (FDM) has been commonly used to numerically solve Richard's equation, numerical difficulties are often encountered, even for simple problems. To minimize convergence problems, comparatively small space discretization and time steps have often been adopted to address the nonlinearity of the problem, resulting in significant computational costs.

A new numerical scheme was developed by Cavalcante and Zornberg (2016) to solve problems involving the advection-dispersion contaminant transport equation. The new scheme was found to successfully address numerical problems typically obtained when solving the advection-dispersion equation using the traditional FDM approach. At least for cases where the seepage velocity in contaminant transport problems is constant, the numerical solution obtained using FDM is conditionally stable. However, Cavalcante and Zornberg (2016) showed that the FDM solution presents spurious numerical dissipation errors when using schemes involving Courant numbers less than 1. This undesirable dissipation effect leads to increasing dumping of the solution for decreasing Courant numbers, which is a necessary condition for convergence while solving numerically certain partial differential equations using finite differences. Consequently, the solution was found to rapidly deteriorate when using small time intervals, which are often adopted to handle the nonlinearity of the problem.

To overcome these difficulties, this paper presents an algorithm for solving Richard's equation by combining two numerical techniques: the FDM and the cubic interpolated pseudoparticle (CIP) method. Codes were developed using *Mathematica* to implement the algorithms developed in this study.

General Approach for Numerical Solution

Differential equations, such as the version of Richard's equation expressed by Eq. (4), can be grouped into distinct components (Hundsdorfer and Verwer 2003). Specifically, Eq. (4) can be considered to include a diffusive component, represented by

$$\frac{\partial \theta}{\partial t} = \frac{\partial}{\partial z}\left[D_z(\theta)\frac{\partial \theta}{\partial z}\right] \tag{6}$$

and an advective component represented by

$$\frac{\partial \theta}{\partial t} = -a_s(\theta)\frac{\partial \theta}{\partial z} \tag{7}$$

Using the time-splitting technique, the rate of moisture changes can be expressed as

$$\frac{\partial \theta}{\partial t} = \frac{\theta_k^{n+1} - \theta_k^{(n+1)^*}}{\Delta t} + \frac{\theta_k^{(n+1)^*} - \theta_k^{n}}{\Delta t} \tag{8}$$

where θ_k^n = volumetric water content for step n and position k; θ_k^{n+1} = volumetric water content for the subsequent step $(n+1)$; and $\theta_k^{(n+1)^*}$ = volumetric water content for an intermediate time $[(n+1)^*]$ that only accounts for the diffusive component of the unsaturated flow process.

The diffusive component can be initially solved considering the initial and boundary conditions of the problem. Specifically, the explicit solution of Eq. (6) for time step $(n+1)^*$ and space step k $\left[\theta_k^{(n+1)^*}\right]$ can be obtained as follows:

$$\frac{\theta_k^{(n+1)^*} - \theta_k^{n}}{\Delta t} = \frac{\partial}{\partial z}\left[D_z(\theta)\frac{\partial \theta}{\partial z}\right] \tag{9}$$

The resulting moisture content $\left[\theta_k^{(n+1)^*}\right]$ can be subsequently used to obtain the solution that also considers the advective component of the unsaturated flow process, as follows:

$$\frac{\theta_k^{n+1} - \theta_k^{(n+1)^*}}{\Delta t} = -a_s(\theta)\frac{\partial \theta}{\partial z} \tag{10}$$

where θ_k^{n+1} = explicit solution of Eq. (7) for time step $(n+1)$ and space step k. θ_k^{n+1} also corresponds to the actual solution of Eq. (4) considering both diffusive and advective components of the unsaturated flow process.

This general algorithm is repeated until the final time (time step n) is reached for each node (space step k). The specific details of the algorithms implemented to numerically solve the diffusive and advective components of Eq. (4) are provided next.

Diffusive Component

Eq. (9) is solved using the FDM, considering an explicit scheme, as follows:

$$\theta_k^{(n+1)^*} = \theta_k^n + \frac{\Delta t}{\Delta z}\left[D_{k+1/2}^n\left(\frac{\partial \theta}{\partial z}\right)_{k+1/2}^n - D_{k-1/2}^n\left(\frac{\partial \theta}{\partial z}\right)_{k-1/2}^n\right] \tag{11}$$

with

$$D^n_{k+1/2} = \frac{1}{2}\left[D_z\left(\theta^n_{k+1}\right) + D_z\left(\theta^n_k\right)\right] \tag{12}$$

$$D^n_{k-1/2} = \frac{1}{2}\left[D_z\left(\theta^n_k\right) + D_z\left(\theta^n_{k-1}\right)\right] \tag{13}$$

where $D_z(\theta^n_{k-1})$, $D_z(\theta^n_k)$, and $D_z(\theta^n_{k+1})$ are updated using Eq. (3).

A second-order derivative (in space) can be estimated at cell face for each time step as follows:

$$\left(\frac{\partial\theta}{\partial z}\right)^n_{k+1/2} = \frac{\theta^n_{k+1} - \theta^n_k}{\Delta z} \tag{14}$$

$$\left(\frac{\partial\theta}{\partial z}\right)^n_{k-1/2} = \frac{\theta^n_k - \theta^n_{k-1}}{\Delta z} \tag{15}$$

The size of the time increment (Δt) is controlled by the Neumann number (N_e), which at each time step n and position k should satisfy the following condition (Smith 1985):

$$N_e = D_z\left(\theta^n_k\right)\frac{\Delta t}{\Delta z^2} \le \frac{1}{2} \tag{16}$$

Advective Component

The CIP method is proposed in this study for solving the advective component of Richard's equation instead of using the more commonly implemented FDM. However, to allow comparison of the predictions obtained using the newly proposed and the traditional approaches, both the FDM and CIP methods were implemented in this study, as discussed in this section.

Finite-Difference Scheme

Using the FDM, Eq. (10) can be discretized using a second-order (in space) estimate for space derivation at cell face for any time step as follows:

$$\theta^{n+1}_k = \theta^{(n+1)^*}_k - \frac{\Delta t}{\Delta z}\left\{a^{(n+1)^*}_{k+1/2}\left[\theta^{(n+1)^*}_{k+1} - \theta^{(n+1)^*}_k\right] - a^{(n+1)^*}_{k-1/2}\left[\theta^{(n+1)^*}_k - \theta^{(n+1)^*}_{k-1}\right]\right\} \tag{17}$$

with

$$a^{(n+1)^*}_{k+1/2} = \frac{1}{2}\left\{a_s\left[\theta^{(n+1)^*}_{k+1}\right] + a_s\left[\theta^{(n+1)^*}_k\right]\right\} \tag{18}$$

$$a^{(n+1)^*}_{k-1/2} = \frac{1}{2}\left\{a_s\left[\theta^{(n+1)^*}_k\right] + a_s\left[\theta^{(n+1)^*}_{k-1}\right]\right\} \tag{19}$$

where $a_s\left[\theta^{(n+1)^*}_{k-1}\right]$, $a_s\left[\theta^{(n+1)^*}_k\right]$, and $a_s\left[\theta^{(n+1)^*}_{k+1}\right]$ are updated using Eq. (5).

The time increment (Δt) is controlled by the Courant number (C_r), which at each time step should satisfy the following condition (Smith 1985):

$$C_r = a_s\left[\theta^{(n+1)^*}_k\right]\frac{\Delta t}{\Delta z} \le 1 \tag{20}$$

CIP Scheme

The CIP method (Takewaki et al. 1985; Takewaki and Yabe 1987) can be used instead of the FDM to eliminate reported spurious numerical dissipation errors (Cavalcante and Zornberg 2016). Specifically, Eq. (7) can be differentiated in relation to z as follows:

$$\frac{\partial}{\partial z}\left(\frac{\partial\theta}{\partial t}\right) = -\frac{\partial}{\partial z}\left[a_s(\theta)\frac{\partial\theta}{\partial z}\right] \tag{21}$$

Applying the chain rule, Eq. (21) can be rewritten as follows:

$$\frac{\partial q}{\partial t} + a_s\frac{\partial q}{\partial z} = -q\frac{\partial a_s}{\partial z} \tag{22}$$

where a_s is given by Eq. (5); and q is defined as

$$q = \frac{\partial\theta}{\partial z} \tag{23}$$

Because a_s is greater than 0, θ^n_k can be approximated by a Hermite cubic polynomial given by (Takewaki et al. 1985; Takewaki and Yabe 1987)

$$F^n_k(z) = \alpha^n_k(z - z^n_k)^3 + \beta^n_k(z - z^n_k)^2 + \chi^n_k(z - z^n_k) + \eta^n_k \tag{24}$$

where

$$\alpha^n_k = \frac{q^n_k + q^n_{k-1}}{\Delta z^2} - \frac{2\left(\theta^{n^*}_k - \theta^{n^*}_{k-1}\right)}{\Delta z^3} \tag{25}$$

$$\beta^n_k = \frac{2q^n_k + q^n_{k-1}}{\Delta z} - \frac{3\left[\theta^{(n+1)^*}_k - \theta^{(n+1)^*}_{k-1}\right]}{\Delta z^2} \tag{26}$$

$$\chi^n_k = q^n_k \tag{27}$$

$$\eta^n_k = \theta^{(n+1)^*}_k \tag{28}$$

The time evolution of the functions θ and q can be obtained by using the following Lagrangian invariants:

$$\theta^{n+1}_k = F^n_k\left\{z^n_k - a_s\left[\theta^{(n+1)^*}_k\right]\Delta t\right\} \tag{29}$$

$$q^{n+1}_k = \frac{\partial}{\partial z}F^n_k\left\{z^n_k - a_s\left[\theta^{(n+1)^*}_k\right]\Delta t\right\} \tag{30}$$

The time increment (Δt) is controlled by the Courant number, which at each time step should satisfy the condition presented in Eq. (20).

It should be noted that all numerical schemes adopted in this study involve explicit solutions. This is important because most FDM schemes reported in the literature [e.g., Celia et al. (1987); Bouloutas (1989); Celia and Bouloutas (1990)] involve implicit solutions, which require comparatively higher computational effort and processing time.

Validation of Numerical Approaches

The analytical solutions obtained by Cavalcante and Zornberg (2017) are used in this section to validate the adequacy of the numerical predictions obtained using the numerical schemes presented in the previous section.

The analytical solutions reported by Cavalcante and Zornberg (2017) were developed using a logarithmic relationship between suction and volumetric water content [$\psi(\theta)$] and a linear relationship between hydraulic conductivity and volumetric water content [$k_z(\theta)$]. Accordingly, $\psi(\theta)$ is represented by

$$\psi(\theta) = \frac{1}{\delta} \ln\left(\frac{\theta - \theta_r}{\theta_s - \theta_r}\right) \tag{31}$$

where θ_s = volumetric water content at saturation (L^3/L^3); θ_r = residual volumetric water content (L^3/L^3); and δ = fitting hydraulic parameter ($M^{-1}LT^2$). The difference between θ_s and θ_r has often been referred to as the soil moisture capacity. In contrast, the unsaturated hydraulic conductivity [$k_z(\theta)$] is given by

$$k_z(\theta) = k_s\left(\frac{\theta - \theta_r}{\theta_s - \theta_r}\right) \tag{32}$$

where k_s = saturated hydraulic conductivity of the soil (L/T).

For these adopted relationships, the hydraulic parameters $D_z(\theta)$ [Eq. (3)] and $a_s(\theta)$ [Eq. (5)] become constants. Specifically, the resulting constant hydraulic parameters are

$$\bar{D}_z = \frac{k_s}{\delta(\theta_s - \theta_r)\rho_w g} \tag{33}$$

$$\bar{a}_s = \frac{k_s}{(\theta_s - \theta_r)} \tag{34}$$

where $\bar{D}_z$ = constant unsaturated water diffusivity in the z-direction; and $\bar{a}_s$ = constant unsaturated advective seepage, as obtained when $\psi(\theta)$ and $k_z(\theta)$ are represented by logarithmic and linear relationships, respectively.

The validation of the proposed numerical schemes conducted in this study included the case of an unsaturated flow problem with an imposed constant discharge velocity (v_0) on the upper boundary of a semi-infinite soil column that is characterized by a constant initial moisture content (θ_i). The analytical solution used herein to validate the numerical scheme involves a semi-infinite soil column, with a constant discharge velocity being imposed on its upper boundary [Case 3, as reported by Cavalcante and Zornberg (2017)]. Specifically, the initial condition for this case is described by a uniform initial moisture content, as follows:

$$\theta(z, 0) = \theta_i \tag{35}$$

where θ_i = constant.

A Neumann flux boundary condition is adopted, which involves a constant discharge velocity imposed on the upper boundary of the domain, as follows:

$$\left(\bar{D}_z \frac{\partial \theta}{\partial z} - k_z\right)\Big|_{z=0} = v_0 \tag{36}$$

where v_0 = constant. The maximum discharge velocity that can be physically imposed corresponds to the soil saturated hydraulic conductivity (k_s). Specifically, the maximum imposed discharge velocity is

$$v_{0,\max} = \frac{\theta_s k_s}{(\theta_s - \theta_r)} \tag{37}$$

For the semi-infinite soil column in this problem, the lower boundary condition adopted in this study is described by

$$\frac{\partial \theta}{\partial z}(\infty, t) = 0 \tag{38}$$

This lower boundary condition implies that, at depth, the moisture content (and consequently, the suction) reaches a constant value. It also implies that, at depth, the hydraulic gradient in the z-direction equals 1. The analytical solution that corresponds to these initial and boundary conditions is (Cavalcante and Zornberg 2017)

$$\theta(z, t) = \theta_i + \left[\frac{v_0}{k_s}(\theta_s - \theta_r) - \theta_i\right] C(z, t) \tag{39}$$

with

$$C(z, t) = \frac{1}{2}\text{erfc}(Z_{-1}) + \sqrt{\frac{\bar{a}_s^2 t}{\pi \bar{D}_z}} \exp\left[-\frac{(z - \bar{a}_s t)^2}{4\bar{D}_z t}\right] - \frac{1}{2}\left(-1 + \frac{\bar{a}_s z}{\bar{D}_z} + \frac{\bar{a}_s^2 t}{\bar{D}_z}\right) \exp\left(\frac{\bar{a}_s z}{\bar{D}_z}\right) \text{erfc}(Z_{+1}) \tag{40}$$

$$Z_{\pm 1} = \frac{z \pm \bar{a}_s t}{2\sqrt{\bar{D}_z t}} \tag{41}$$

where erfc(Z) = complementary error function, defined as

$$\text{erfc}(Z) = 1 - \frac{2}{\pi} \int_0^Z \exp\left(-t^2\right) dt \tag{42}$$

The analytical solutions to this problem are initially compared to the numerical predictions obtained using the previously discussed FDM scheme. Specifically, both the diffusive and the advective flow components [Eqs. (6) and (7)] are initially solved using FDM. The analytical solutions are subsequently compared to the numerical predictions obtained using combined FDM/CIP schemes as proposed in this study. That is, the FDM is used to solve the diffusive flow component [Eq. (6)], and the CIP method is used to solve the advective flow component [Eq. (7)].

The same discretizations of time and space were adopted for the numerical simulations conducted using each of the two numerical schemes evaluated in this study (i.e., FDM and FDM/CIP). The values of the soil hydraulic parameters θ_i, θ_r, θ_s, k_s, and δ adopted in this evaluation are 0.13, 0.04, 0.41, 8.2×10^{-7} m/s, and 0.03 kPa^{-1}, respectively. Figs. 1(a and b) illustrate the logarithmic SWRC and the linear k-function, expressed in terms of ψ, that correspond to the adopted hydraulic parameters. The k-function presented in Fig. 1(b) illustrates that, even though this function is linear when expressed in terms of θ, it shows an exponential trend when expressed in terms of ψ. The shape of the hydraulic functions presented in Fig. 1 is consistent with generally reported trends in experimental data, which usually show a nonlinear relationship with ψ.

The initial condition adopted in this validation involves a uniform moisture content ($\theta_i = 0.13$). The constant discharge velocity imposed on the upper boundary of the semi-infinite column is $v_0 = 2.10^{-7}$ m/s.

For the conditions in this problem, the time increment (Δt) adopted in this validation should satisfy the following condition for the diffusive component of the unsaturated flow [Eq. (16)]:

$$\Delta t \leq \frac{1}{2}\frac{\Delta z^2}{k_s} \delta \rho_w g(\theta_s - \theta_r) \tag{43}$$

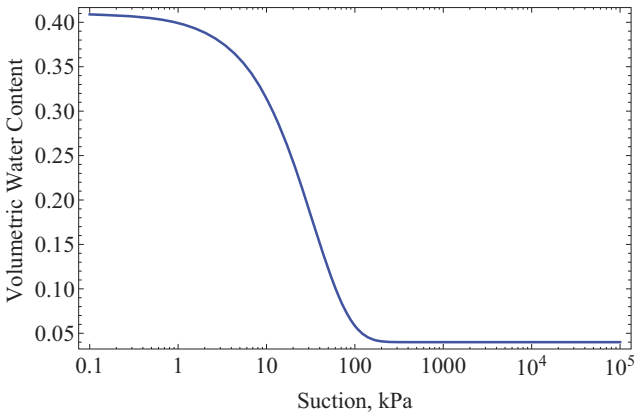

(a)

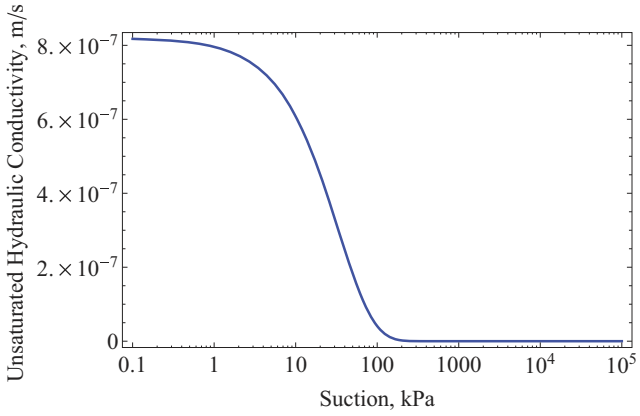

(b)

Fig. 1. Unsaturated hydraulic functions used for validation: (a) logarithmic SWRC; (b) linear k-function ($\delta = 0.03\,\text{kPa}^{-1}$)

Also, the adopted increment Δt should satisfy the following condition for the advective component of the flow [Eq. (20)]:

$$\Delta t \leq \frac{\Delta z}{k_s}(\theta_s - \theta_r) \tag{44}$$

The numerical solution was obtained considering time step Δt = 64 s and space step Δz = 0.001 m. The adopted discretization satisfies the convergence criteria defined by Eqs. (43) and (44) (N_e = 0.48; C_r = 0.14). The domain involved 675,000 nodes, corresponding to 500 space increments, and the total time in the simulation is 24 h, which corresponds to 1,350 time increments.

Fig. 2 shows the comparison between analytical solutions [Eq. (39)] and numerical predictions obtained using FDM [Eqs. (11) and (17)]. The results are presented as moisture profiles for increasing periods of time (4, 14, and 24 h). The numerical predictions obtained using the FDM scheme are found to show some numerical spuriusness, which led to a comparatively poor agreement with the analytical solution.

Fig. 3 shows the comparison between analytical results [Eq. (39)] and numerical predictions obtained using the FDM/CIP scheme [Eqs. (11) and (29)]. The results are also presented as moisture profiles for increasing periods of time (4, 14, and 24 h). The discretization in time and space is the same as that used for the FDM approach. The numerical predictions obtained using the FDM/CIP scheme show a very good agreement with the analytical results.

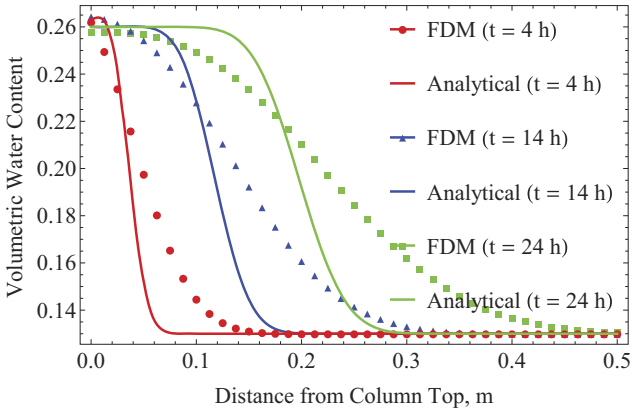

Fig. 2. Comparison between analytical solution and numerical predictions using the FDM scheme

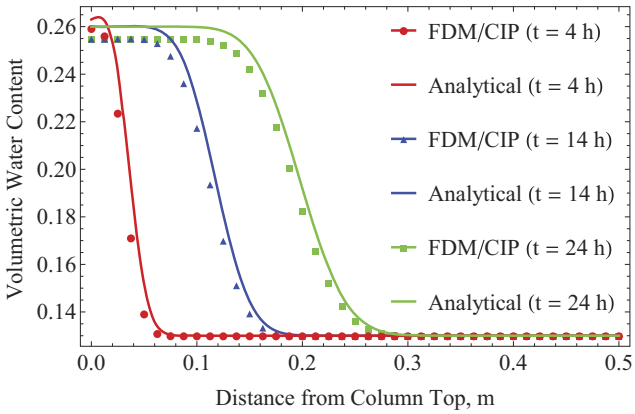

Fig. 3. Comparison between analytical solution and numerical predictions using the FDM/CIP scheme

In addition to the comparisons presented in Figs. 2 and 3, additional evaluations were conducted to compare the analytical results against the numerical predictions using a variety of initial and boundary conditions. Specifically, the additional analyses involved cases corresponding to a constant moisture imposed on the upper boundary of a semi-infinite column, a constant moisture imposed on the upper boundary of a column of finite length, and a constant discharge velocity imposed on the upper boundary of a column of finite length. These additional cases were selected for comparison, as they correspond to boundary conditions for which analytical solutions are now available (Cavalcante and Zornberg 2017). In all cases, the numerical predictions obtained using the FDM/CIP scheme showed better agreement with the analytical results than the numerical predictions obtained using the FDM.

General Framework for Solving Unsaturated Flow Problems Using Multiple Models for Hydraulic Functions

The validation of the proposed numerical scheme, as conducted in this study and presented in the previous section, involved numerical predictions using hydraulic functions for which transient analytical solutions have been developed (Cavalcante and Zornberg 2017). After the completion of such validation, the numerical approach

involving the use of a FDM/CIP scheme is extended in this section to allow use of hydraulic functions for which no closed-form analytical solutions are readily available. Specifically, rather than adopting the logarithmic and linear functions for the SWRC and k-function, respectively, a variety of other functions commonly adopted in practice and reported in the technical literature [e.g., Gardner (1958); Brooks and Corey (1964); van Genuchten (1980)] are implemented herein.

For the different hydraulic functions, which are often defined in terms of suction (ψ), it becomes initially necessary to define them in terms of θ—that is, to define the SWRC in the form $\psi(\theta)$ and the k-function in the form $k_z(\theta)$. This allows the subsequent determination of the functions $D_z(\theta)$ and $a_s(\theta)$, which are needed to implement the proposed numerical approach.

For example, the van Genuchten model (and most other models) is typically represented using ψ as an independent variable [i.e., $\theta(\psi)$] rather than using θ as an independent variable [i.e., $\psi(\theta)$]. Accordingly, the soil water retention defined using van Genuchten's model (van Genuchten 1980) in the form $\theta(\psi)$ can be represented in the form $\psi(\theta)$, as follows:

$$\psi(\theta) = \frac{1}{\alpha_{r,\mathrm{vg}}} \sqrt[n_{r,\mathrm{vg}}]{\sqrt[m_{r,\mathrm{vg}}]{\left(\frac{\theta-\theta_r}{\theta_s-\theta_r}\right)^{-1}} - 1} \tag{45}$$

where $\alpha_{r,\mathrm{vg}}$, $n_{r,\mathrm{vg}}$, and $m_{r,\mathrm{vg}}$ = fitting van Genuchten's parameters (van Genuchten 1980), with the parameter $m_{r,\mathrm{vg}}$ defined as

$$m_{r,\mathrm{vg}} = 1 - \frac{1}{n_{r,\mathrm{vg}}} \tag{46}$$

The subscript r adopted throughout this paper indicates that the fitting parameter corresponds to a retention curve (i.e., relationship between θ and ψ). The subscript vg adopted throughout this paper indicates that the fitting parameter corresponds to the van Genuchten (1980) model.

Also, the k-function defined using van Genuchten's model (van Genuchten 1980) in the form $k_z(\psi)$, can be redefined in the form $k_z(\theta)$ as follows:

$$k_z(\theta) = k_s \sqrt{\frac{\theta-\theta_r}{\theta_s-\theta_r}} \left\{ 1 - \left[1 - \left(\frac{\theta-\theta_r}{\theta_s-\theta_r} \right)^{\frac{1}{m_{k,\mathrm{vg}}}} \right]^{m_{k,\mathrm{vg}}} \right\}^2 \tag{47}$$

where k_s = saturated hydraulic conductivity (L/T); and $m_{k,\mathrm{vg}}$ = fitting van Genuchten's parameter (van Genuchten 1980), which has been reported as

$$m_{k,\mathrm{vg}} = 1 - \frac{1}{n_{k,\mathrm{vg}}} \tag{48}$$

where $n_{k,\mathrm{vg}}$ = another fitting van Genuchten's parameter (van Genuchten 1980). The subscript k adopted throughout this paper indicates that the fitting parameter corresponds to a hydraulic conductivity function (k-function).

It should be noted that van Genuchten's model, as reported by van Genuchten (1980), considers $m_{k,\mathrm{vg}} = m_{r,\mathrm{vg}}$ and $n_{k,\mathrm{vg}} = n_{r,\mathrm{vg}}$. However, the formulation presented in this paper does not impose that the hydraulic parameters of the SWRC necessarily be the same as those of the k-function. This is expected to facilitate the use of the formulations developed in this paper in problems where both the SWRC and the k-function have been defined experimentally (rather than the common approach of only using experimental data to define the SWRC).

For the case of a soil with hydraulic functions $\psi(\theta)$ and $k_z(\theta)$ represented using the van Genuchten model, the function $D_z(\theta)$ was subsequently obtained using Eqs. (3), (45), and (47). The resulting unsaturated water diffusivity [$D_z(\theta)$] for the van Genuchten model is

$$D_z(\theta) = -\frac{k_s \Phi^2 \left(-1 + \Phi^{-1/m_{r,\mathrm{vg}}}\right)^{-1+\frac{1}{n_{r,\mathrm{vg}}}} \Phi^{-\frac{2+m_{r,\mathrm{vg}}}{2m_{r,\mathrm{vg}}}}}{m_{r,\mathrm{vg}}\, n_{r,\mathrm{vg}}\, \alpha_{r,\mathrm{vg}}\, \rho_w\, g(\theta_s-\theta_r)} \tag{49}$$

with

$$\Phi = \frac{\theta-\theta_r}{\theta_s-\theta_r} \tag{50}$$

where Φ = normalized volumetric water content.

Also, the function $a_s(\theta)$ can be obtained using Eqs. (5) and (47). Accordingly, the unsaturated advective seepage for the van Genuchten model is

$$a_s(\theta) = -\frac{k_s}{2(\theta-\theta_r)(\theta-\theta_s)} \Phi\sqrt{\Phi} \times \left[\theta(4-5\Phi) - 4\theta_r(1-\Phi) + \theta_s\Phi\right] \tag{51}$$

Unlike the case reported by Cavalcante and Zornberg (2017), where the hydraulic functions are defined using a simple logarithmic function for $\psi(\theta)$ and a linear function for $k_z(\theta)$ [Eqs. (31) and (32), respectively], an analytical solution is not available for the case where the hydraulic functions are defined using the van Genuchten model. Even for the steady-state condition, the analytical solution for this problem has not been obtained. For the common cases for which analytical solutions are not available, the efficient FDM/CIP approach developed in this paper provides an efficient framework for solving unsaturated flow problems numerically.

Eqs. (52)–(55) present the soil water retention models proposed by Gardner (1958), Brooks and Corey (1964), van Genuchten (1980), and the model used in the analytical solutions (Cavalcante and Zornberg 2017), respectively. The three initial models have been extensively used in unsaturated flow problems, whereas the last model is the one for which analytical solutions are available. The form of the SWRC indicated as $\Phi(\psi)$ in Eqs. (52)–(55) corresponds to the form of these functions [$\Phi(\psi)$ or $\theta(\psi)$] as originally represented by their authors

$$\Phi(\psi) = (1 + \alpha_{r,\mathrm{g}}\psi^{n_{r,\mathrm{g}}})^{-1} \tag{52}$$

$$\Phi(\psi) = (\alpha_{r,\mathrm{bc}}\psi)^{-\lambda_{r,\mathrm{bc}}} \tag{53}$$

$$\Phi(\psi) = [1 + (\alpha_{r,\mathrm{vg}}\psi)^{n_{r,\mathrm{vg}}}]^{-m_{r,\mathrm{vg}}} \tag{54}$$

$$\Phi(\psi) = e^{-\delta_{r,\mathrm{cz}}|\psi|} \tag{55}$$

Subscript r indicates that the fitting parameter is for a SWRC. Subscripts g, bc, vg, and cz indicate that the fitting parameter corresponds to the Gardner (1958), Brooks and Corey (1964), van Genuchten (1980), or Cavalcante and Zornberg (2017) models, respectively. Eqs. (56)–(59) provide the inverse of these functions [$\psi(\Phi)$], which corresponds to the form of the SWRC used in the formulations presented in this paper. An analytical solution for

Cavalcante and Zornberg (2017) is available, but only for $\delta_{k,cz} = \delta_{r,cz} = \delta$

$$\psi(\Phi) = \sqrt[n_{r,g}]{\frac{1-\Phi}{\alpha_{r,g}\Phi}} \tag{56}$$

$$\psi(\Phi) = \frac{\Phi^{-1/\lambda_{r,bc}}}{\alpha_{r,bc}} \tag{57}$$

$$\psi(\Phi) = \frac{1}{\alpha_{r,vg}} \sqrt[n_{r,vg}]{\Phi^{-1/m_{r,vg}} - 1} \tag{58}$$

$$\psi(\Phi) = \frac{1}{\delta_{r,cz}} \ln(\Phi) \tag{59}$$

Eqs. (60)–(63) present the k-function models proposed by Gardner (1958), Brooks and Corey (1964), van Genuchten (1980), and Cavalcante and Zornberg (2017), respectively. The three initial models have also been extensively used to solve unsaturated flow problems, whereas the last model is the one for which analytical solutions are available. The form of the k-function indicated as $k_z(\psi)$ in Eqs. (60)–(63) corresponds to the form of these functions as they were originally represented by their authors

$$k_z(\psi) = k_s e^{-\alpha_{k,g}\psi} \tag{60}$$

$$k_z(\psi) = k_s(\alpha_{k,bc}\psi)^{-\beta_{k,bc}} \tag{61}$$

$$k_z(\psi) = \frac{k_s\sqrt{\left[1+(\alpha_{k,vg}\psi)^{n_{k,vg}}\right]^{-m_{k,vg}}}}{\left[1-\left(\left\{1-\left[1+(\alpha_{k,vg}\psi)^{n_{k,vg}}\right]^{-m_{k,vg}}\right\}^{\frac{1}{m_{k,vg}}}\right)^{m_{k,vg}}\right]^{-2}} \tag{62}$$

$$k_z(\psi) = k_s \exp\left(-\delta_{k,cz}|\psi|\right) \tag{63}$$

Subscript k indicates that the fitting parameter is for an unsaturated k-function. Eqs. (64)–(67) provide the correspondent k-function in terms of θ—that is, the function $k_z(\Phi)$, which corresponds to the form of the k-function used in the formulations presented in this paper

$$k_z(\Phi) = k_s e^{-\alpha_{k,g}\left(\frac{1-\Phi}{\alpha_{r,g}\Phi}\right)^{\frac{1}{n_{r,g}}}} \tag{64}$$

$$k_z(\Phi) = k_s\left(\frac{\alpha_{k,bc}}{\alpha_{r,bc}}\Phi^{-1/\lambda_{r,bc}}\right)^{-\beta_{k,bc}} \tag{65}$$

$$k_z(\Phi) = \frac{k_s\sqrt{\Phi}}{\left\{1-\left[(1-\Phi)^{\frac{1}{m_{k,vg}}}\right]^{m_{k,vg}}\right\}^{-2}} \tag{66}$$

$$k_z(\Phi) = k_s\Phi \tag{67}$$

Using derivations similar to those illustrated for the case of the van Genuchten model, $D_z(\theta)$ and $a_s(\theta)$ were derived for the various constitutive models listed in Eqs. (52)–(67). Accordingly, Eqs. (68) and (69) present the functions $D_z(\theta)$ and $a_s(\theta)$ as derived for the case of Gardner (1958). The hydraulic parameters for the SWRC presented in Eqs. (68) and (69) for the Gardner (1958) model are not considered to be necessarily the same as the hydraulic parameters for the k-function

$$D_z(\theta) = -\frac{e^{-\alpha_{k,g}\left[\frac{-\theta+\theta_s}{\alpha_{r,g}(\theta-\theta_r)}\right]^{\frac{1}{n_{r,g}}}} k_s(\theta_r-\theta_s)\left[\frac{-\theta+\theta_s}{\alpha_{r,g}(\theta-\theta_r)}\right]^{\frac{1}{n_{r,g}}}}{n_{r,g}(\theta-\theta_r)(\theta-\theta_s)\rho_w g} \tag{68}$$

$$a_s(\theta) = \frac{e^{-\alpha_{k,g}\left[\frac{-\theta+\theta_s}{\alpha_{r,g}(\theta-\theta_r)}\right]^{\frac{1}{n_{r,g}}}} k_s\alpha_{k,g}(\theta_r-\theta_s)\left[\frac{-\theta+\theta_s}{\alpha_{r,g}(\theta-\theta_r)}\right]^{\frac{1}{n_{r,g}}}}{n_{r,g}(\theta-\theta_r)(\theta-\theta_s)} \tag{69}$$

Eqs. (70) and (71) present the functions $D_z(\theta)$ and $a_s(\theta)$ for the case of the Brooks and Corey (1964) model

$$D_z(\theta) = -\frac{k_s\left[\frac{\alpha_{k,bc}}{\alpha_{r,bc}}\left(-\frac{\theta-\theta_r}{\theta_r-\theta_s}\right)^{-1/\lambda_{r,bc}}\right]^{1-\beta_{k,bc}}}{\alpha_{k,bc}\,\lambda_{r,bc}\,\rho_w g(\theta-\theta_r)} \tag{70}$$

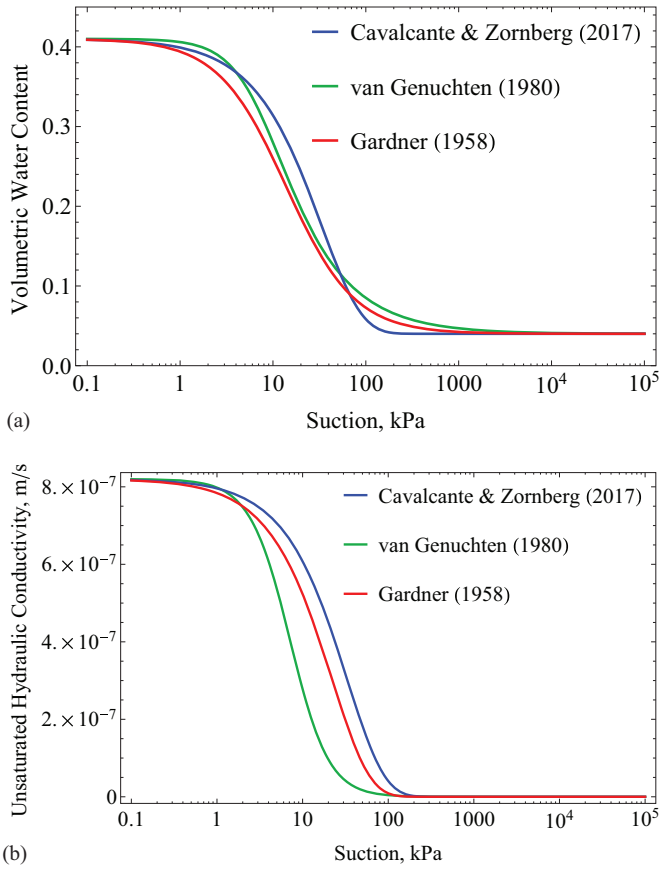

Fig. 4. Hydraulic functions by Gardner (1958) and van Genuchten (1980) obtained as best fit to those defined by Cavalcante and Zornberg (2017) in the comparative example: (a) SWRCs; (b) k-function models

$$a_s(\theta) = \frac{k_s \beta_{k,\mathrm{bc}} \left[\dfrac{\alpha_{k,\mathrm{bc}}}{\alpha_{r,\mathrm{bc}}} \left(\dfrac{-\theta + \theta_r}{\theta_r - \theta_s} \right)^{-1/\lambda_{r,\mathrm{bc}}} \right]^{-\beta_{k,\mathrm{bc}}}}{(\theta - \theta_r)\lambda_{r,\mathrm{bc}}} \tag{71}$$

Appendixes I and II provide a summary of the various functions of $D_z(\theta)$ and $a_s(\theta)$. These functions were obtained using Eqs. (3) and (5) for the various combinations of soil water retention models presented in Eqs. (56)–(59) and k-function models presented in Eqs. (64)–(67). The results are presented in the appendixes, and they correspond to the multiple possible combinations involving use of models. The various functions were obtained considering that the fit parameters of SWRC and k-function may be different.

Because analytical solutions are available for the case of the Cavalcante and Zornberg (2017) model, the good comparison between the numerical predictions and the analytical solutions presented in the previous section provides validation of the numerical scheme proposed in this paper. Analytical solutions are not available to provide such rigorous validation of numerical implementations that use other commonly adopted models presented in Eqs. (52)–(67). However, an approximate validation could also be conducted for the case of the hydraulic functions developed by Gardner (1958) and van Genuchten (1980). This was achieved by identifying the parameters from these models that provide a good fit to the hydraulic functions that have been defined using the hydraulic parameter (δ) proposed by Cavalcante and Zornberg (2017) (Fig. 1). This approach allows comparison of the numerical predictions obtained using the Gardner (1958) and van Genuchten (1980) models against analytical solutions obtained using Cavalcante and Zornberg (2017) hydraulic functions.

Fig. 4 shows a comparison of the soil SWRCs and the k-functions adopted in this evaluation for the log-linear, Gardner, and van Genuchten models. The parameters $\delta_{r,\mathrm{cz}} = \delta_{k,\mathrm{cz}} = 0.03\,\mathrm{kPa}^{-1}$ in the log-linear model (Cavalcante and Zornberg 2017) were found to define a SWRC and a k-function that are well represented by parameters $\alpha_{r,\mathrm{g}} = 0.004$, $n_{r,g} = 1.78$, and $\alpha_{k,\mathrm{g}} = 0.035$ for the Gardner (1958) model, and by parameters $\alpha_{r,\mathrm{vg}} = 0.13$, $n_{r,\mathrm{vg}} = 1.88$, and $n_{k,\mathrm{vg}} = 1.88$ for the van Genuchten (1980) model.

The initial condition used in this evaluation was a uniform initial moisture content of 0.13 and a constant discharge velocity of 2×10^{-7} m/s applied to the upper boundary of the domain. The volumetric water content at saturation, residual volumetric water content, and the saturated hydraulic conductivity were 0.41, 0.04, and 8.2×10^{-7} m/s, respectively.

Figs. 5–7 provide a comparison of the analytical results (obtained using the Cavalcante and Zornberg model) with the numerical predictions obtained using the Gardner (1958) and van Genuchten (1980) models. The numerical predictions were obtained using the FDM/CIP scheme proposed in this paper. The same mesh used in the validation presented in the previous section was adopted in this comparison—that is, 675,000 nodes corresponding to 500 space increments and 1,350 time increments (Δt = 64 s, $\Delta z = 0.001$ m).

Fig. 5(a) illustrates the time history of the transient volumetric water content results, obtained at different locations within the soil column. The results were obtained numerically using the FDM/CIP scheme for the case of the Gardner (1958) and van Genuchten

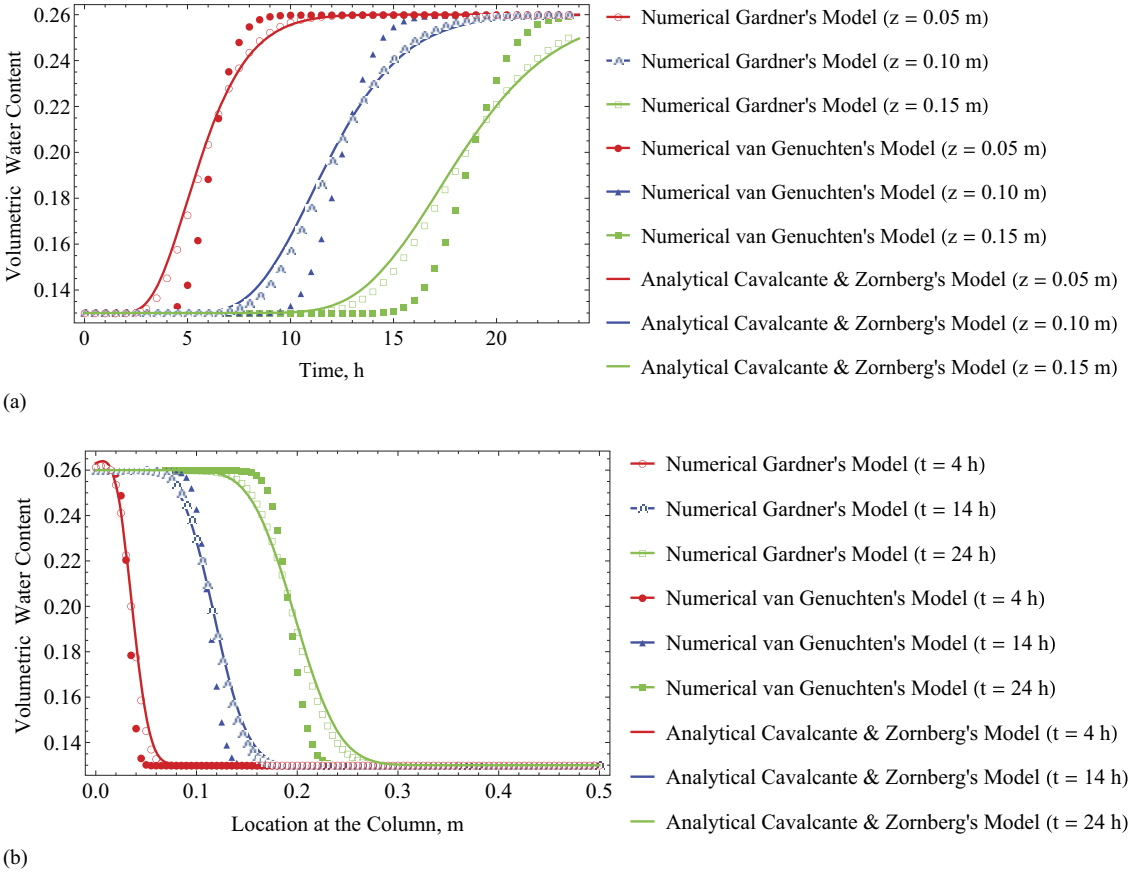

Fig. 5. Comparison of the analytical solution (Cavalcante and Zornberg model) and the numerical predictions (Gardner and van Genuchten models) for volumetric water content: (a) time history at different locations; (b) moisture profiles at different times

(1980) models, and analytically for the case of the Cavalcante and Zornberg (2017) model. The results in Fig. 5(a) illustrate that the volumetric water content in the unsaturated soil column increases nonlinearly as time increases until reaching the ultimate moisture content of 0.26. The results in Fig. 5(a) also show that the volumetric water content increases at a faster rate near the top of the soil column.

Fig. 5(b) provides a comparison of the numerical predictions of the moisture profiles at increasing time for the Gardner (1958) and van Genuchten (1980) models, in relation to the analytical results obtained for the Cavalcante and Zornberg (2017) model. Fig. 5(b) shows that the volumetric water content in an unsaturated soil is lower when far from the upper boundary condition during the infiltration process.

More importantly, the results in the figure indicate that the numerical predictions obtained using the FDM/CIP scheme for the Gardner (1958) and van Genuchten (1980) models compare very well with the analytical results obtained for the Cavalcante and Zornberg (2017) model. Any minor discrepancies between numerical predictions and analytical results are attributed to differences among the hydraulic functions adopted for the different simulations. In fact, the better comparison between the prediction by the Gardner (1958) model and the analytical results is consistent with the better fit between the Gardner (1958) hydraulic function and the Cavalcante and Zornberg (2017) hydraulic functions (Fig. 4).

Fig. 6(a) illustrates the time history of the transient total suction results, obatined at different locations within the soil column. The results were obtained numerically using the FDM/CIP scheme for the case of the Gardner (1958) and van Genuchten (1980) models, and analytically for the case of the Cavalcante and Zornberg (2017) model. The results in Fig. 6(a) show that the total suction in the unsaturated soil decreases nonlinearly as time increases until reaching saturation. Fig. 6(a) also illustrates that the total suction decreases at a faster rate near the top of the soil column.

Fig. 6(b) provides a comparison of the numerical predictions of the total suction profiles at increasing time for the Gardner (1958) and van Genuchten (1980) models in relation to the predicted results obtained for the Cavalcante and Zornberg (2017) model. Fig. 6(b) illustrates that the total suction in an unsaturated soil is higher when far from the upper boundary condition, as expected, because the infiltration process happens in a soil column with constant initial moisture.

Overall, the evaluation provided in this section indicates that the proposed FDM/CIP scheme leads to very accurate predictions of the transient response of unsaturated flow. In particular, these results confirm the adequacy of the values of diffusivity and advective seepage, developed as part of this study for a number of hydraulic models reported in the literature.

Fig. 7(a) illustrates the time history of the transient unsaturated hydraulic conductivity results obtained at different locations within the soil column. The results were obtained numerically using the FDM/CIP scheme for the case of the Gardner (1958) and van Genuchten (1980) models, and anallytically for the case of the Cavalcante and Zornberg (2017) model. The results in Fig. 7(a) illustrate that the hydraulic conductivity in the unsaturated soil column increases nonlinearly as the time increases to saturation. The results in Fig. 7(a) also show that the hydraulic conductivity increases at a faster rate near the top of the soil column.

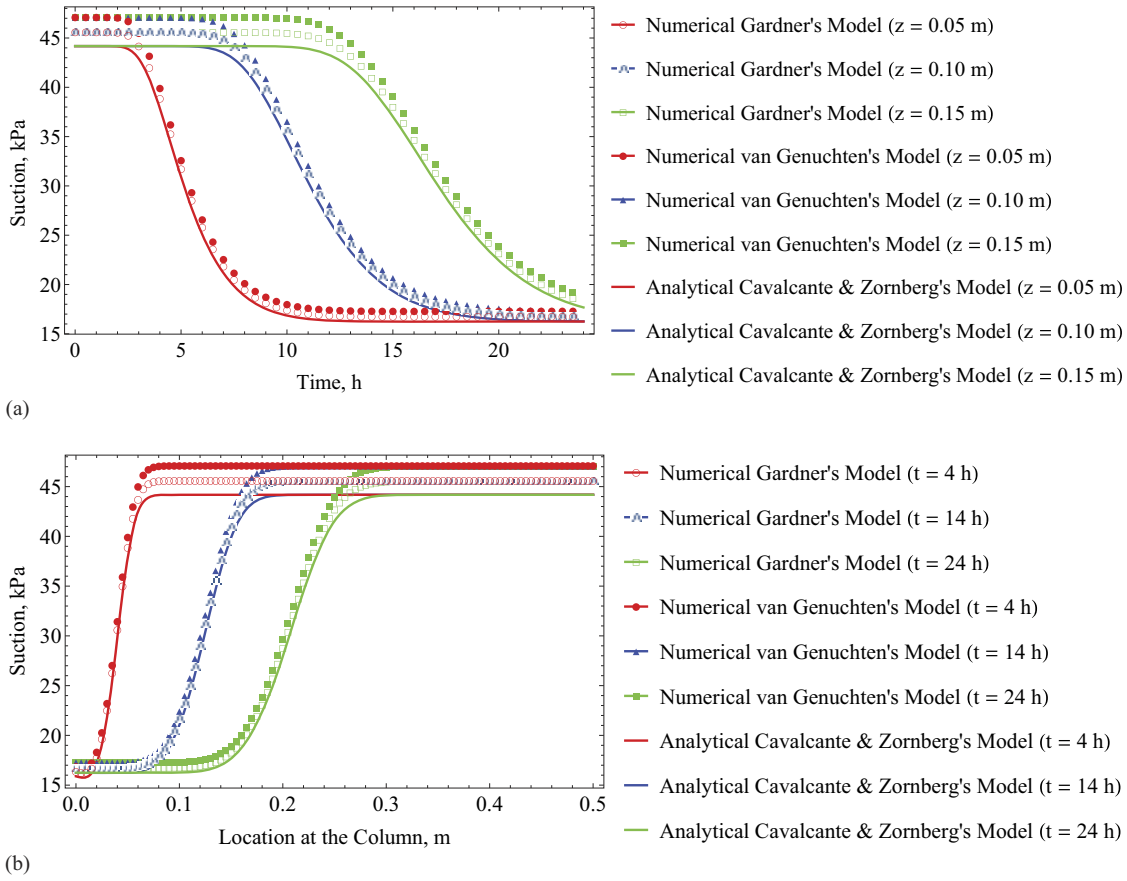

Fig. 6. Comparison of the analytical solution (Cavalcante and Zornberg model) and the numerical predictions (Gardner and van Genuchten models) for suction: (a) time history at different locations; (b) suction profiles at different times

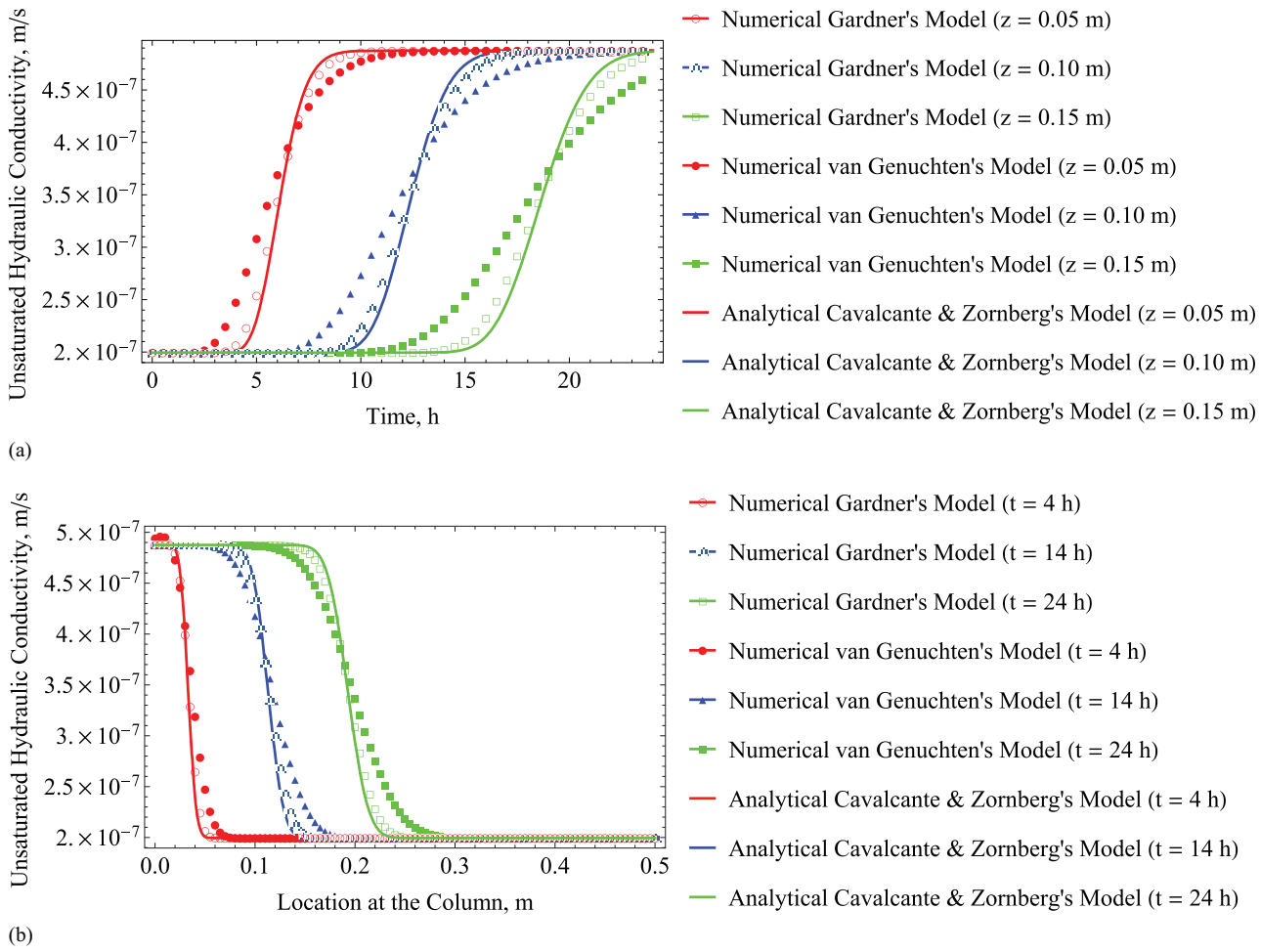

Fig. 7. Comparison of the analytical solution (Cavalcante and Zornberg model) and the numerical predictions (Gardner and van Genuchten models) for unsaturated hydraulic conductivity: (a) time history at different locations; (b) permeability profiles at different times

Fig. 7(b) provides a comparison of the numerical predictions of the unsaturated hydraulic conductivity profiles at increasing time for the Gardner (1958) and van Genuchten (1980) models in relation to the analytical results obtained for the Cavalcante and Zornberg (2017) model. Fig. 7(b) illustrates that the hydraulic conductivity in an unsaturated soil is lower when far from the upper boundary condition, as expected, because the soil has a higher suction much deeper.

Conclusions

The objective of this paper was to develop an efficient numerical approach to solving Richard's equation by combining two numerical techniques: the FDM and the CIP method. This numerical effort capitalizes on the availability of analytical solutions of Richard's equations for unsaturated flow under transient conditions, which are presented in a companion paper (Cavalcante and Zornberg 2017). The numerical solution allowed validation of the proposed numerical schemes not only for the case of hydraulic models (i.e., SWRCs, *k*-functions) for which analytical solutions had been developed, but also for conventional hydraulic models. The following specific conclusions can be drawn based on the numerical developments, evaluations, and validations conducted as part of this study:

- The use of a form of Richard's equation that allows identification of diffusive and advective flow components was found to be particularly appropriate for implementation of the CIP method to solve the advective flow component.
- The FDM was found to be adequate for solving the diffusion component of Richard's equation, which could be controlled by adopting time steps corresponding to Neumann's number below 0.5.
- The CIP method was found to be suitable for facilitating convergence and eliminate the presence of spurious results (e.g., numerical dissipation trends in the predictions) when Courant's number is less than 1.0.
- Use of a new hybrid (FDM/CIP) algorithm was found to be particularly accurate and stable for solving Richard's equation, particularly when compared to the more traditional use of FDM techniques.
- The good comparison between numerical predictions and analytical solutions for flow problems conducted using boundary conditions and hydraulic functions, for which transient analytical solutions are available (Cavalcante and Zornberg 2017), allowed validation of the numerical scheme proposed in this paper.
- The new numerical approach could be extended to solve unsaturated flow problems involving comparatively complex soil hydraulic functions as well as different boundary conditions. Specifically, the diffusivity and advective seepage terms needed for numerical implementation were developed for the Gardner (1958), Brooks and Corey (1964), and van Genuchten (1980) models.

- Evaluations were conducted to compare numerical predictions using hydraulic functions for which no analytical solutions are available. Comparisons of numerical predictions using hydraulic functions that fit well those for which analytical solutions are available confirmed the accuracy of the proposed numerical scheme for commonly used hydraulic models.

Overall, the newly developed algorithm was found to be particularly accurate and stable for solving Richard's equation, being clearly superior to the use of the traditional FDM.

Appendix I. Function $a_s(\theta)$

Eqs. (72)–(75) present a summary of the various functions of $a_s(\theta)$. These functions were obtained using Eq. (5) for the various k-function models proposed by Gardner (1958), Brooks and Corey (1964), van Genuchten (1980), and Cavalcante and Zornberg (2017), respectively

$$a_s(\theta) = \frac{e^{-\alpha_{k,g}\left[\frac{-\theta+\theta_s}{\alpha_{r,g}(\theta-\theta_r)}\right]^{\frac{1}{n_{r,g}}}} k_s(\theta_r-\theta_s)\left[\frac{-\theta+\theta_s}{\alpha_{r,g}(\theta-\theta_r)}\right]^{\frac{1}{n_{r,g}}}}{n_{r,g}(\theta-\theta_r)(\theta-\theta_s)} \tag{72}$$

$$a_s(\theta) = \frac{k_s\beta_{k,bc}\left[\frac{\alpha_{k,bc}}{\alpha_{r,bc}}\left(\frac{-\theta+\theta_r}{\theta_r-\theta_s}\right)^{-1/\lambda_{r,bc}}\right]^{-\beta_{k,bc}}}{(\theta-\theta_r)\lambda_{r,bc}} \tag{73}$$

$$\begin{aligned} a_s(\theta) = {} & \frac{k_s}{2(\theta-\theta_r)(\theta-\theta_s)}\left\{-1+\left[\left(\frac{\theta-\theta_s}{\theta_r-\theta_s}\right)^{\frac{1}{m_{k,vg}}}\right]^{m_{k,vg}}\right\} \\ & \times\sqrt{\frac{-\theta+\theta_r}{\theta_r-\theta_s}}\times\left(\theta\left\{-1+5\left[\left(\frac{\theta-\theta_s}{\theta_r-\theta_s}\right)^{\frac{1}{m_{k,vg}}}\right]^{m_{k,vg}}\right\}\right. \\ & -4\theta_r\left[\left(\frac{\theta-\theta_s}{\theta_r-\theta_s}\right)^{\frac{1}{m_{k,vg}}}\right]^{m_{k,vg}}+\theta_s \\ & \left.-\left[\left(\frac{\theta-\theta_s}{\theta_r-\theta_s}\right)^{\frac{1}{m_{k,vg}}}\right]^{m_{k,vg}}\theta_s\right) \end{aligned} \tag{74}$$

$$a_s(\theta) = \frac{k_s}{\theta_s-\theta_r} \tag{75}$$

Appendix II. Function $D_z(\theta)$

Eqs. (76)–(79) provide a summary of the various functions of $D_z(\theta)$. These functions were obtained using Eq. (3) for the various combinations of soil water retention model presented by Gardner (1958) and k-function models proposed by Gardner (1958), Brooks and Corey (1964), van Genuchten (1980), and Cavalcante and Zornberg (2017), respectively

$$D_z(\theta) = -\frac{e^{-\alpha_{k,g}\left[\frac{-\theta+\theta_s}{\alpha_{r,g}(\theta-\theta_r)}\right]^{\frac{1}{n_{r,g}}}} k_s(\theta_r-\theta_s)\left[\frac{-\theta+\theta_s}{\alpha_{r,g}(\theta-\theta_r)}\right]^{\frac{1}{n_{r,g}}}}{n_{r,g}(\theta-\theta_r)(\theta-\theta_s)\rho_w g} \tag{76}$$

$$D_z(\theta) = -\frac{e^{-\alpha_{k,g}\left[-\frac{\theta-\theta_s}{\alpha_{r,g}(\theta-\theta_r)}\right]^{\frac{1}{n_{r,g}}}} k_s\left(-\frac{\theta-\theta_r}{\theta_r-\theta_s}\right)^{-\frac{1}{\lambda_{r,bc}}}}{\rho_w g\alpha_{r,bc}\lambda_{r,bc}(\theta-\theta_r)} \tag{77}$$

$$D_z(\theta) = \frac{e^{-\alpha_{k,g}\left[\frac{-\theta+\theta_s}{\alpha_{r,g}(\theta-\theta_r)}\right]^{\frac{1}{n_{r,g}}}} k_s\left[-1+\left(\frac{-\theta+\theta_r}{\theta_r-\theta_s}\right)^{-1/m_{r,vg}}\right]^{\frac{1}{n_{r,vg}}}}{m_{r,vg}\,n_{r,vg}\,\alpha_{r,vg}(\theta-\theta_r)\left[-1+\left(\frac{-\theta+\theta_r}{\theta_r-\theta_s}\right)^{1/m_{r,vg}}\right]\rho_w g} \tag{78}$$

$$D_z(\theta) = -\frac{e^{-\alpha_{k,g}}k_s\left[-\frac{\theta-\theta_s}{\alpha_{r,g}(\theta-\theta_r)}\right]^{\frac{1}{n_{r,g}}}}{\delta_{r,cz}\,\rho_w g(\theta-\theta_r)} \tag{79}$$

Eqs. (80)–(83) also provide a summary of the various functions of $D_z(\theta)$. These functions were obtained using Eq. (3) for the various combinations of soil water retention model presented by Brooks and Corey (1964) and k-function models proposed by Gardner (1958), Brooks and Corey (1964), van Genuchten (1980), and Cavalcante and Zornberg (2017), respectively

$$D_z(\theta) = -\frac{k_s\left[\frac{\alpha_{k,bc}}{\alpha_{r,bc}}\left(-\frac{\theta-\theta_r}{\theta_r-\theta_s}\right)^{-1/\lambda_{r,bc}}\right]^{-\beta_{k,bc}}(\theta_r-\theta_s)\left[-\frac{\theta-\theta_s}{\alpha_{r,g}(\theta-\theta_r)}\right]^{\frac{1}{n_{r,g}}}}{n_{r,g}(\theta-\theta_r)(\theta-\theta_s)\rho_w g} \tag{80}$$

$$D_z(\theta) = -\frac{k_s\left[\frac{\alpha_{k,bc}}{\alpha_{r,bc}}\left(\frac{-\theta+\theta_r}{\theta_r-\theta_s}\right)^{-1/\lambda_{r,bc}}\right]^{1-\beta_{k,bc}}}{\alpha_{k,bc}\,\lambda_{r,bc}(\theta-\theta_r)\rho_w g} \tag{81}$$

$$D_z(\theta) = \frac{k_s\left[-1+\left(\frac{-\theta+\theta_r}{\theta_r-\theta_s}\right)^{-1/m_{r,vg}}\right]^{\frac{1}{n_{r,vg}}}\left[\frac{\alpha_{k,bc}}{\alpha_{r,bc}}\left(\frac{-\theta+\theta_r}{\theta_r-\theta_s}\right)^{-1/\lambda_{r,bc}}\right]^{-\beta_{k,bc}}}{m_{r,vg}\,n_{r,vg}\,\alpha_{r,vg}(\theta-\theta_r)\left[-1+\left(\frac{-\theta+\theta_r}{\theta_r-\theta_s}\right)^{\frac{1}{m_{r,vg}}}\right]\rho_w g} \tag{82}$$

$$D_z(\theta) = \frac{k_s \left[\frac{\alpha_{k,\mathrm{bc}}}{\alpha_{r,\mathrm{bc}}} \left(-\frac{\theta - \theta_r}{\theta_r - \theta_s} \right)^{-1/\lambda_{r,\mathrm{bc}}} \right]^{-\beta_{k,\mathrm{bc}}}}{\delta_{r,\mathrm{cz}}(\theta - \theta_r)\rho_w g} \tag{83}$$

Eqs. (84)–(87) present a summary of the various functions of $D_z(\theta)$. These functions were obtained using Eq. (3) for the various combinations of soil water retention model presented by van Genuchten (1980) and *k*-function models proposed by Gardner (1958), Brooks and Corey (1964), van Genuchten (1980), and Cavalcante and Zornberg (2017), respectively

$$D_z(\theta) = \frac{-\left(k_s \left\{ -1 + \left[\left(\frac{\theta - \theta_s}{\theta_r - \theta_s} \right)^{1/m_{k,\mathrm{vg}}} \right]^{m_{k,\mathrm{vg}}} \right\}^2 \sqrt{\frac{-\theta + \theta_r}{\theta_r - \theta_s}} \, (\theta_r - \theta_s) \left[\frac{-\theta + \theta_s}{\alpha_{r,\mathrm{g}}(\theta - \theta_r)} \right]^{\frac{1}{n_{r,\mathrm{g}}}} \right)}{n_{r,\mathrm{g}}(\theta - \theta_r)(\theta - \theta_s)\rho_w g} \tag{84}$$

$$D_z(\theta) = \frac{k_s \left\{ -1 + \left[\left(\frac{\theta - \theta_s}{\theta_r - \theta_s} \right)^{1/m_{k,\mathrm{vg}}} \right]^{m_{k,\mathrm{vg}}} \right\}^2 \left(\frac{-\theta + \theta_r}{\theta_r - \theta_s} \right)^{-\frac{2+\lambda_{r,\mathrm{bc}}}{2\lambda_{r,\mathrm{bc}}}}}{\alpha_{r,\mathrm{bc}}(\theta_r - \theta_s)\lambda_{r,\mathrm{bc}} \, \rho_w g} \tag{85}$$

$$D_z(\theta) = -\frac{k_s \left\{ -1 + \left[\left(\frac{\theta - \theta_s}{\theta_r - \theta_s} \right)^{\frac{1}{m_{k,\mathrm{vg}}}} \right]^{m_{k,\mathrm{vg}}} \right\}^2 \left[-1 + \left(\frac{-\theta + \theta_r}{\theta_r - \theta_s} \right)^{-1/m_{r,\mathrm{vg}}} \right]^{-1+1/n_{r,\mathrm{vg}}} \left(\frac{-\theta + \theta_r}{\theta_r - \theta_s} \right)^{-\frac{2+m_{r,\mathrm{vg}}}{2m_{r,\mathrm{vg}}}}}{m_{r,\mathrm{vg}} \, n_{r,\mathrm{vg}} \, \alpha_{r,\mathrm{vg}}(\theta_s - \theta_r)\rho_w g} \tag{86}$$

$$D_z(\theta) = -\frac{k_s \left\{ -1 + \left[\left(\frac{\theta - \theta_s}{\theta_r - \theta_s} \right)^{1/m_{k,\mathrm{vg}}} \right]^{m_{k,\mathrm{vg}}} \right\}^2 \sqrt{\frac{-\theta + \theta_r}{\theta_r - \theta_s}}}{\delta_{r,\mathrm{cz}}(\theta - \theta_r)\rho_w g} \tag{87}$$

Finally, Eqs. (88)–(91) also present a summary of the various functions of $D_z(\theta)$. These functions were obtained using Eq. (3) for the various combinations of soil water retention model presented by Cavalcante and Zornberg (2017) and *k*-function models proposed by Gardner (1958), Brooks and Corey (1964), van Genuchten (1980), and Cavalcante and Zornberg (2017), respectively

$$D_z(\theta) = \frac{k_s \left[-\frac{\theta - \theta_s}{\alpha_{r,\mathrm{g}}(\theta - \theta_r)} \right]^{\frac{1}{n_{r,\mathrm{g}}}}}{n_{r,\mathrm{g}}(\theta - \theta_s)\rho_w g} \tag{88}$$

$$D_z(\theta) = \frac{k_s \left(-\frac{\theta - \theta_r}{\theta_r - \theta_s} \right)^{-1/\lambda_{r,\mathrm{bc}}}}{\alpha_{r,\mathrm{bc}} \, \lambda_{r,\mathrm{bc}}(\theta_r - \theta_s)\rho_w g} \tag{89}$$

$$D_z(\theta) = -\frac{k_s \left[-1 + \left(\frac{-\theta + \theta_r}{\theta_r - \theta_s} \right)^{-\frac{1}{m_{r,\mathrm{vg}}}} \right]^{\frac{1}{n_{r,\mathrm{vg}}}}}{m_{r,\mathrm{vg}} \, n_{r,\mathrm{vg}} \, \alpha_{r,\mathrm{vg}} \left[-1 + \left(\frac{-\theta + \theta_r}{\theta_r - \theta_s} \right)^{\frac{1}{m_{r,\mathrm{vg}}}} \right] (\theta_r - \theta_s)\rho_w g} \tag{90}$$

$$D_z(\theta) = \frac{k_s}{\delta_{r,\mathrm{cz}}(\theta_r - \theta_s)\rho_w g} \tag{91}$$

Acknowledgments

The authors acknowledge the support of the following institutions: the National Council for Scientific and Technological Development (CNPq Project 30449420127), the Coordination for the Improvement of Higher Level Personnel (CAPES Project 1431/14-5), the National Science Foundation (CMMI Grant 1335456), the University of Brasilia, and the University of Texas, Austin, for funding this research.

References

Bear, J. (1979). *Hydraulics of groundwater*, McGraw-Hill, New York.

Bouloutas, E. T. (1989). "Improved numerical approximations for flow and transport in the unsaturated zone." Ph.D. thesis, Dept. of Civil Engineering, Massachusetts Institute of Technology, Cambridge, MA.

Brooks, R. H., and Corey, A. T. (1964). *Hydraulic properties of porous media*, Colorado State Univ., Fort Collins, CO.

Cavalcante, A. L. B., and Zornberg, J. G. (2016). "Numerical schemes to solve advective contaminant transport problems with linear sorption and first order decay." *Electron. J. Geotech. Eng.*, 21(5), 2043–2060.

Cavalcante, A. L. B., and Zornberg, J. G. (2017). "Efficient approach to solving transient unsaturated flow problems. I: Analytical solutions." *Int. J. Geomech.*, 10.1061/(ASCE)GM.1943-5622.0000875, 04017013.

Celia, M. A., Ahuja, L. R., and Pinder, G. F. (1987). "Orthogonal collocation and alternating-direction procedures for unsaturated flow problems." *Adv. Water Resour.*, 10(4), 178–187.

Celia, M. A., and Bouloutas, E. T. (1990). "A general mass-conservative numerical solution for the unsaturated flow equation." *Water Resour. Res.*, 26(7), 1483–1496.

Gardner, W. R. (1958). "Some steady state solutions of the unsaturated moisture flow equation with application to evaporation from a water table." *Soil Sci.*, 85(4), 228–232.

Hundsdorfer, W. H., and Verwer, D. B. (2003). "Numerical solution of time-dependent advection-diffusion-reaction equations." *Springer series in computational mathematics*, Vol. 33, Springer, New York.

Mathematica [Computer software]. Wolfram, Champaign, IL.

Philip, J. R. (1969). "Theory of infiltration." *Advances in hydroscience*, V. T. Chow, ed., Vol. 5, Academic Press, New York, 215–296.

Richards, L. A. (1931). "Capillary conduction of liquids through porous mediums." *J. Appl. Phys.*, 1(5), 318–333.

Smith, G. D. (1985). *Numerical solution of partial differential equations: Finite difference methods*, 3rd Ed., Oxford University Press, New York, 67–68.

Takewaki, H., Nishiguchi, A., and Yabe, T. (1985). "Cubic interpolated pseudo-particle method (CIP) for solving hyperbolic-type equations." *J. Comput. Phys.*, 61(2), 261–268.

Takewaki, H., and Yabe, T. (1987). "The cubic-interpolated pseudo particle (CIP) method: Application to nonlinear and multi-dimensional hyperbolic equations." *J. Comput. Phys.*, 70(2), 355–372.

Van Genuchten, M. T. (1980). "A closed form equation for predicting the hydraulic conductivity of unsaturated soils." *Soil Sci. Am. J.*, 44(5), 892–898.